Journal of Materials Chemistry

Cite this: *J. Mater. Chem.*, 2012, **22**, 932

www.rsc.org/materials

PAPER

Synthesis of multifunctional polymer brush surfaces *via* sequential and orthogonal thiol-click reactions†

Santosh B. Rahane,[a] Ryan M. Hensarling,[a] Bradley J. Sparks,[a] Christopher M. Stafford[b] and Derek L. Patton*[a]

Received 23rd September 2011, Accepted 27th October 2011
DOI: 10.1039/c1jm14762e

Fabrication of multifunctional surfaces with complexity approaching that found in nature requires the application of a modular approach to surface engineering. We describe a versatile post-polymerization modification strategy to synthesize multifunctional polymer brush surfaces *via* combination of surface-initiated photopolymerization (SIP) and orthogonal thiol-click reactions. Specifically, we demonstrate two routes to multifunctional brush surfaces: in the first approach, alkyne-functionalized homopolymer brushes are modified with multiple thiols *via* a statistical, radical-mediated thiol-yne co-click reaction; and in the second approach, statistical copolymer brushes carrying two distinctly-addressable reactive moieties are sequentially modified *via* orthogonal base-catalyzed thiol-X (where X represents an isocyanate, epoxy, or α-bromoester) and radical-mediated thiol-yne reactions. In both cases, we show that surface properties, in the form of wettability, can be easily tuned over a wide range by judicious choice of brush composition and thiol functionality.

Introduction

Multicomponent surfaces - where all components synergistically control the surface properties - are ubiquitous in natural biological systems. For example, the unique superhydrophobic properties of lotus leaves, butterfly wings, and rose petals result from not only multi-scale surface topographies, but also cooperative interactions of these features with multicomponent chemical compositions.[1] The allure of mimicking nature's approach to surface engineering - particularly the ability to install multiple chemical functionalities on surfaces in a controlled fashion - has recently attracted significant attention in terms of strategies leading to multifunctional surfaces and advanced applications in biosensors, self-cleaning surfaces, *etc.* Among several immobilization strategies reported for surface modification, those that exploit "click" reactions, such as the azide-alkyne Huisgen 1,3-dipolar cycloaddition,[2,3] Diels–Alder,[4–6] and thiol-click,[7–10] as well as other high efficiency transformations like activated ester-amine reactions,[11–13] are particularly attractive for the fabrication of multifunctional surfaces. These reactions - due to the possibility of orthogonal reaction conditions - permit sequential and/or simultaneous modifications resulting in the ability to control the number and spatial location of multiple functional groups on the surface.[3,14,15] Orthogonal modification of surfaces using Cu(I)-catalyzed azide-alkyne Huisgen 1,3-dipolar cycloaddition (CuAAC) has been demonstrated by several groups. For example, Murphy *et al.*[16] simultaneously immobilized amine and acetylene-terminated peptides onto a mixed self-assembled monolayer containing complementary carboxylate and azide groups *via* orthogonal carbodiimide condensation and CuAAC chemistry to create multifunctional surfaces that present distinct peptides to stem cells on a bioinert background. These surfaces enabled a better understanding of multiple, distinct extracellular factors that work in concert to regulate stem cell adhesion at interfaces. Im *et al.*[17] used orthogonal acetylene and amine functionalized thin films obtained by plasma enhanced chemical vapor deposition for synthesis of multifunctional nanopatterned surfaces *via* an elegant one-pot transformation using CuAAC and carbodimide/activated ester chemistries. Concern over the presence of residual metal impurities following copper-catalyzed click reactions has motivated the development of alternate, metal-free surface modification strategies. Consequently, a wide variety of metal-free click reactions - such as strain promoted azide-alkyne cycloadditions,[18–21] and Diels–Alder cycloadditions[4–6] - are increasingly becoming methods of choice to synthesize multifunctional surfaces *via* orthogonal transformations. For example, Orski and coworkers[22] used cyclopropenone-masked dibenzocyclooctynes tethered on a brush surface for light-activated and orthogonal immobilization of two azides *via* sequential copper-free [3 + 2] cycloaddition click reactions. Similarly, a route to bio-orthogonal multifunctional surface modification using copper-free azide-alkyne click with electron-deficient alkynes was recently demonstrated by Deng *et al.*[23]

Alternatively, we and others have shown thiol-based click reactions - such as thiol-ene,[24–28] thiol-yne[27,29–33] and thiol-isocyanate[34,35] - to be

[a]*School of Polymers and High Performance Materials, University of Southern Mississippi, Hattiesburg, Mississippi, 39406, USA*
[b]*Polymers Division, National Institute of Standards and Technology, Gaithersburg, Maryland, 20899, USA*
† Electronic supplementary information (ESI) available. See DOI: 10.1039/c1jm14762e

a powerful approach for engineering multifunctional materials and surfaces in a modular fashion. Thiol-click reactions are advantageous for this purpose in that they proceed at room temperature with high efficiency and rapid kinetics, in the presence of oxygen/water, without expensive and potentially toxic catalysts, and are highly tolerant of a wide range of functional groups. Additionally, thiol-click reactions are orthogonal to a wide range of chemistries.[36] Notably, one only has to look within the thiol-click class of reactions to realize a powerful set of orthogonal transformations that enable the installation of multiple chemical functionalities on a surface with high efficiency and modularity. Herein, we describe a versatile post-polymerization modification strategy to synthesize multifunctional polymer brush surfaces *via* combination of surface-initiated photopolymerization (SIP) and orthogonal thiol-click reactions. One of the principal advantages of the post-modifiable brush platform is that it provides a much larger number of modifiable sites per unit area of substrate as compared to conventional self-assembled monolayers (SAMs), while decoupling the polymer synthesis step from the immobilization of sensitive functional groups on the surface thereby avoiding expensive monomer synthesis and reducing potential side reactions.[37] Specifically, we demonstrate two routes to multifunctional brush surfaces: In the first approach, alkyne-functionalized homopolymer brushes are simultaneously modified with multiple thiols *via* a statistical, radical-mediated thiol-yne co-click reaction; and in the second approach, copolymer brushes carrying two distinctly-addressable reactive moieties are sequentially modified *via* orthogonal base-catalyzed thiol-X (where X represents an isocyanate, epoxy,[38] or α-bromoester[39–41]) and radical-mediated thiol-yne reactions. In both cases, we show that surface properties, in the form of wettability as a model example, can be easily tuned over a wide range by judicious choice of brush composition and thiol functionality.

Experimental section

Materials and methods

Certain commercial materials and equipment are identified in the paper in order to adequately specify the experimental details. In no case does such identification imply recommendation by the National Institute of Standards and Technology nor does it imply that the material or equipment identified is necessarily the best available for the purpose. All the solvents and reagents were obtained at the highest purity available from Aldrich Chemical Company or Fisher Scientific and were used as received unless otherwise specified. Silicon wafers polished only on one side were purchased from University Wafers. Commercially available photoinitiator, 2-hydroxy-4′-(2-hydroxyethoxy)-2-methyl-propiophenone (Irgacure 2959), was obtained from Ciba Specialty Chemicals and modified with trichlorosilane according to a previously reported protocol.[29,42]

Monomers, glycidyl methacrylate (GMA; Acros Organics, 97%), hydroxyethylmethacrylate (HEMA, 98% Aldrich), and 2-isocyanatoethyl methacrylate (NCOMA; TCI America, 98%), were passed through basic and vacuum-dried neutral alumina columns, respectively, to remove the inhibitor. Protected propargyl alcohol, 3-trimethylsilylpropargyl alcohol (PgOH-TMS; 98%), was purchased from GFS Chemicals and was used as received. All thiols were obtained at the highest available purity from Aldrich Chemical Company and were used without any further purification. Reagents, 1,8-diazabicyclo[5.4.0]undec-7-ene (DBU) and 2,2-dimethoxy-2-phenyl acetophenone (DMPA), for thiol-click reactions were also obtained from Aldrich and used as received.

Synthesis of protected alkyne containing monomer, (3-trimethylsilylpropargyl) methacrylate (PgMA-TMS). PgMA-TMS was synthesized according to a previously reported protocol.[29] Briefly, PgMA-TMS was synthesized by reacting 1 equivalent of PgOH-TMS with 1.2 equivalents of methacryloyl chloride in presence of 1.2 molar equivalents of triethylamine in CH_2Cl_2. First, methacryloyl chloride was added dropwise to the mixture of PgOH-TMS and triethyl amine cooled in an ice bath. The reaction mixture was stirred for 1 h at 0 °C and then at room temperature overnight. The salt byproducts were filtered and the filtrate was washed with deionized water, saturated sodium carbonate and brine, and the organic layer was dried over $MgSO_4$. The product was finally concentrated using rotavap distillation and purified by column chromatography (silica gel column with 40 : 1 hexane:acetone as eluent) to obtain pure PgMA-TMS (73 % yield). ^{1}H-NMR ($CDCl_3$; δ (ppm)): 0.19 (s, 9H, Si(C^8H_3)$_3$), 1.97 (s, 3H, C^3H_3), 4.76 (s, 2H, C^5H_2), 5.62 (s, 1H, C^1HH), 6.18 (s, 1H, C1H*H*); ^{13}C-NMR ($CDCl_3$; δ (ppm)): 1.76, 20.41, 55.1, 94.2, 101.3, 128.7, 137.9, 168.9. Anal. Calculated for $C_{10}H_{16}O_2Si$: C, 61.18; H, 8.21; O, 16.30; Si, 14.31; Found: C 60.96; H 8.19. (+ESI-MS) *m*/*z* (%): 219 [M + Na] (100), 197 [MH^+] (40). IR (neat): ν ~ = 2960, 1723, 1638, 1452, 1366, 1314, 1292, 1251, 1147, 1035, 971, 942, 842, 813, 761 cm^{-1}.

Synthesis of α-bromoester containing monomer, 2-(2-bromopropanoyloxy) ethyl methacrylate (BrMA). BrMA was synthesized by reacting 1 equivalent of HEMA with 1.1 equivalents of 2-bromopropionyl bromide in presence of 1 molar equivalents of triethylamine in anhydrous CH_2Cl_2. First, 2-bromopropionyl bromide was added dropwise to the mixture of HEMA and triethyl amine cooled in an ice bath. The reaction mixture was stirred for 1 h at 0 °C and then at room temperature for 4 h. The salt byproducts were filtered and the filtrate was washed with deionized water and saturated sodium carbonate, and the organic layer was dried over $MgSO_4$. The product was finally concentrated using rotavap distillation and purified by column chromatography (silica gel column with 3 : 1 v/v hexane: ethyl acetate as eluent) to obtain pure BrMA in 70 % yield. ^{1}H-NMR ($CDCl_3$; δ (ppm)): 1.79 (d, 3H); 1.92 (s, 3H); 4.37 (m, 5H); 5.57 (s, 1H); 6.11 (s, 1H). ^{13}C-NMR ($CDCl_3$; δ (ppm)): 18.4, 21.8, 39.9, 62.3, 63.8, 126.5, 136.1, 167.3, 170.3. Anal. Calculated for $C_9H_{13}BrO_4$: C, 40.78; H, 4.94; Found: C 40.62; H, 5.09. IR (neat): ν ~ = 2929, 1147, 1718, 1388, 940, 645 cm^{-1}.

Immobilization of 2-hydroxy-4′-(2-hydroxyethoxy)-2-methyl-propiophenone trichlorosilane (HPP-$SiCl_3$) on SiO_2 surfaces. Silicon wafers were cut into appropriate sized pieces and ultrasonically cleaned in acetone, ethanol, and toluene for 15 min in each solvent. The substrates were dried under a stream of N_2 and treated with UV-ozone for 45 min. HPP-$SiCl_3$ (4 mM) in toluene was immobilized on the SiO_2 surface at room temperature using excess triethylamine as an acid scavenger for ~ 1 h. The samples were then cleaned by extensively rinsing with toluene and methanol and dried under a stream of N_2. The acetate protecting

group was removed by immersing the wafers prepared above in a suspension of 240 mg K_2CO_3 in 12 mL methanol containing 150 μL H_2O for 1 h. The substrate was subsequently washed with water, methanol, and toluene followed by drying with a stream of N_2. The functionalized silicon wafers were stored in toluene at −20 °C until use. Ellipsometric thickness of the immobilized photoinitiator was 1.1 nm ± 0.3 nm.

Synthesis of (co)polymer brushes by surface-initiated photopolymerization. All (co)polymer brushes were synthesized by surface-initiated photopolymerization from a solution of the monomer or a mixture of monomers in an appropriate solvent in a custom-built and inert (nitrogen) atmosphere using a microchannel reaction device (fabricated from Norland 81 optical adhesive). This microchannel device uses only 400 μL of monomer solution for a 10 mm × 60 mm substrate and is especially useful for expensive and custom-made monomers. For the sake of brevity, the details of this microchannel-SIP procedure are described elsewhere.[29,43] SIP was carried out using a UV light source (λ_{max} = 365 nm, Omnicure Series 1000 with a 5 mm collimating adaptor) at a light intensity of 150 mW cm^{-2} for a specified time. The synthesized (co)polymer brushes were typically sonicated in a good solvent to remove any physisorbed (co)polymer chains, dried with a stream of nitrogen and stored until further use. A brush thickness of 25 nm was targeted to allow facile characterization by grazing-angle attenuated total reflection FTIR. For trimethylsilyl-protected poly(propargyl methacrylate) (p(PgMA-TMS)) brushes, the TMS group was removed by immersing the wafer in KOH (0.6 g) in methanol (12 mL) at ambient temperature for 1 h to afford the alkyne functionalized polymer brush. The substrate was subsequently washed with water, methanol, toluene, and dried under a stream of N_2. Similarly, silver triflate (AgOTf) in THF/water (1 : 1 v/v) was used to remove the TMS group from brush substrates with base labile linkages (*i.e.* thiourethanes).

Thiol-click reactions on (co)polymer brushes. All thiol-click reactions were conducted under ambient air, temperature and humidity conditions as described in our previous publications.[29,34] DBU (500 : 1 thiol:DBU mol/mol) was used as a catalyst for all base-catalyzed thiol-click reactions and DMPA (2% by mass with respect to the thiol) was used as a source of radicals for all the light-induced thiol-yne reactions. Unless otherwise specified, nucleophile-mediated thiol-click reactions were conducted overnight, only to ensure complete reaction. All thiol-yne reactions were conducted using a UV light source (λ_{max} = 365 nm, Omnicure Series 1000 with a 5 mm collimating adaptor) at a light intensity of 40 mW cm^{-2} for a specified time. The (co) polymer brushes were sonicated in THF after thiol-click reactions to remove unreacted thiols.

Characterization

Chemical structures of synthesized monomers were confirmed using a Varian Mercury Plus 200MHz NMR spectrometer operating at a frequency of 200.13 MHz. VNMR 6.1C software was used for proton and carbon analysis. Ellipsometric measurements were carried out using a Gaertner Scientific Corporation LSE ellipsometer with a 632.8 nm laser at 70° from the normal. Refractive index values of 3.86, 1.45, 1.43 and 1.5 for silicon, oxide layer, photoinitiator monolayer and all polymer layers, respectively, were used to build the layer model and calculate layer thicknesses.[42,44] Wettability of the polymer brush surfaces modified with various functionalities was tracked by measuring static water contact angles using a ramé-hart 200-00 Std.-Tilting B with 10 μL water droplets. The static contact angle goniometer was operated in combination with accompanying DROPimage Standard software. The chemical nature of the polymer brush surfaces was characterized by Fourier transform infrared spectroscopy (FTIR) in grazing-angle attenuated total reflectance mode (gATR-FTIR) using a ThermoScientific FTIR instrument (Nicolet 8700) equipped with a VariGATR™ accessory (grazing angle 65°, germanium crystal; Harrick Scientific). Spectra were collected with a resolution of 4 cm^{-1} by accumulating a minimum of 128 scans per sample. All spectra were collected while purging the VariGATR™ attachment and FTIR instrument with N_2 gas along the infrared beam path to minimize the peaks corresponding to atmospheric moisture and CO_2. Spectra were analyzed and processed using Omnic software. XPS measurements were performed using a Kratos AXIS Ultra DLD Spectrometer (Kratos Analytical, Manchester, UK) with a monochromatic Al K X-ray source (1486.6 eV) operating at 150 W under 1.0 × 10^{-9} Torr. Measurements were performed in hybrid mode using electrostatic and magnetic lenses, and the pass energy of the analyzer was set at 20 eV for high-resolution spectra and 160 eV for survey scans, with energy resolutions of 0.1 eV and 0.5 eV, respectively. Generally, total acquisition times of 180 s and 440 s were used to obtain high resolution and survey spectra, respectively. All XPS spectra were recorded using the Kratos Vision II software; data files were translated to VAMAS format and processed using the CasaXPS software package (v. 2.3.12). Binding energies were calibrated with respect to C 1s at 285 eV.

Results and discussion

One-pot thiol-yne reactions for dual-/multifunctional surfaces

Scheme 1 shows the general schematic for the synthesis of dual-functional polymer brush surfaces using a one-pot thiol-alkyne functionalization of a poly(propargyl methacrylate) (p(PgMA)) brush in the presence of a mixture of thiols. This facile synthesis of dual-functional polymer surfaces is accessible due to the similar reactivity of various thiols with the pendant alkyne groups of the p(PgMA) brush. Fairbanks *et al.*[45] recently showed no statistical difference between the reaction rates of aliphatic thiols and mercaptopropionates with various alkynes under photopolymerization conditions; thus, a one-pot approach would enable a simple route to obtain dual-functional polymer brush surfaces where the final composition of the brush surface depends on the composition of the initial functional thiol mixture used in the thiol-yne reaction. This approach, using a single thiol, was demonstrated previously by our group where it was observed that model thiols reacted quantitatively with alkyne groups within 8 min under the investigated conditions. Similar reaction conditions were adopted here in the case of multiple thiol compositions.

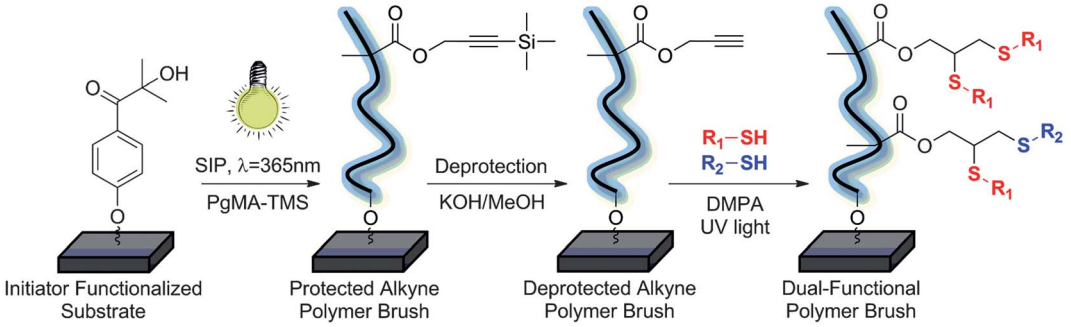

Scheme 1 General schematic for dual-functional polymer brushes by one-pot thiol-yne co-click reactions from PgMA brushes (DMPA = 2,2-Dimethoxy-2-phenylacetophenone). Based on similar thiol reactivities, the thiol-yne co-click reaction yields a distribution of 1,2-homo and 1,2-hetero dithioether adducts within the brush surface.

p(PgMA-TMS) brushes were synthesized by surface-initiated photopolymerization as previously described using the trimethylsilyl-protected alkyne monomer and subsequently deprotected using KOH/methanol to give the terminal alkyne.[29] Fig. 1 (a) and 1(b) show the gATR-FTIR spectra for p(PgMA) brush with pendant alkyne groups in protected and deprotected forms,

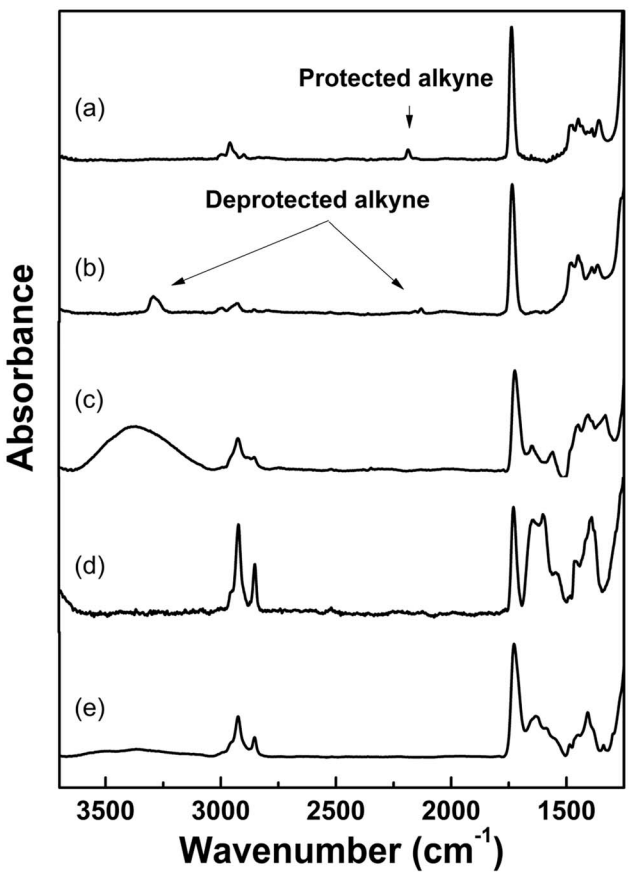

Fig. 1 Poly(propargyl methacrylate) brush a) protected, 23.7 nm ± 1.1 nm; b) deprotected, 11.4 nm ± 1.1 nm; c) clicked with an equimolar mixture of thioglycerol and dodecanethiol, 26.1 nm ± 3.0 nm; d) clicked with an equimolar mixture of dodecanethiol and *N*-acetyl cysteine, 26.9 nm ± 2.3 nm; and e) clicked with an equimolar mixture of dodecanethiol, mercaptopropionic acid and *N*-acetyl cysteine, 26.8 nm ± 2.8 nm.

respectively. The peak at 2189 cm^{-1} for the protected alkyne group in Fig. 1a, and the peaks at 2125 and 3280 cm^{-1} for the deprotected alkyne in Fig. 1b are consistent with our previous work and confirm the successful synthesis of the p(PgMA) brush. The deprotected p(PgMA) brush was further functionalized *via* radical-mediated thiol-yne click by exposing the surface to UV light in the presence of a photoinitiator and a mixture of desired thiols (thiol:THF, 50/50 v/v). All thiol-yne reactions were conducted for 4 h at 40 mW cm^{-2}. The reaction time of 4 h was selected to ensure complete conversion of alkyne groups of p(PgMA) regardless of the fact that the actual time required for complete conversion may be significantly shorter than 4 h. Indeed, quantitative conversion of the alkyne groups was observed following thiol-yne click reactions with equimolar mixtures of various thiols as indicated by the disappearance of the peaks corresponding to deprotected alkyne at 2125 cm^{-1} and 3280 cm^{-1} (gATR-FTIR spectra in Fig. 1c–e). The p(PgMA) brushes showed an expected increase in thickness after thiol-yne reactions with all of the thiol mixtures due to increase in molecular mass of repeat units and was consistent with previous results.[29] Fig. 1c shows the gATR-FTIR spectrum for a p(PgMA) brush after thiol-yne click from an equimolar mixture of dodecanethiol and thioglycerol. As shown in Fig. 1(c), the broad peak between 3600 and 3100 cm^{-1} corresponding to the hydroxyl groups of thioglycerol, and peaks at 2955, 2922 and 2853 cm^{-1} corresponding to the aliphatic chain of dodecanethiol appear indicating that both thiols simultaneously undergo thiol-yne click reaction with p(PgMA) brush. The concentration of the hydrophilic hydroxyl and hydrophobic aliphatic groups in the clicked brush can be easily controlled by simply varying the concentration of respective thiols to control the wettability of the surface. As a second example, we selected a binary mixture of N-acetyl cysteine, a biologically relevant thiol, and dodecanethiol to perform the one-pot thiol-yne click reaction with a p(PgMA) brush. Fig. 1(d) shows the gATR-FTIR spectrum of a p(PgMA) brush clicked with the equimolar mixture of N-acetyl-cysteine and dodecanethiol. Peaks at 1643 cm^{-1} and 1605 cm^{-1} for the secondary amine groups of N-acetyl cysteine, and peaks at 2955 cm^{-1}, 2922 cm^{-1} and 2853 cm^{-1} corresponding to the aliphatic chains of dodecanethiol appear suggesting successful simultaneous thiol-yne click reaction of both the thiols. The one-pot thiol-yne click approach can be further extended to more complex model systems *via* use of ternary thiol mixtures. Fig. 1(e)

shows the gATR-FTIR spectrum of p(PgMA) functionalized with an equimolar ternary mixture of thiols containing dodecanethiol to impart hydrophobic character, 3-mercaptopropionic acid (MPA) to impart hydrophilic character and N-acetyl cysteine as a model biological thiol. As can be observed in Fig. 1 (e), each of the thiols was successfully coupled with the p(PgMA) brush in one-pot fashion: peaks at 2955 cm^{-1}, 2922 cm^{-1} and 2853 cm^{-1} confirm the functionalization with dodecanethiol; the broad peak at 3250 cm^{-1} confirms the functionalization with 3-mercaptopropionic acid; and peaks at 1643 cm^{-1} and 1605 cm^{-1} confirm the successful coupling of N-acetyl cysteine. In principle, this ternary brush surface constitutes a model for a biological molecule embedded in a microenvironment with tunable wettability by virtue of the facile control over the proportion of MPA and dodecanethiol in the ternary thiol mixture.

To demonstrate control over brush composition and ultimately wettability, we modified the p(PgMA) brush *via* thiol-yne reactions with mixtures containing different molar ratios of 3-mercaptopropionic acid and dodecanethiol. Fig. 2 (a–c) shows the gATR-FTIR spectra for polymer brushes clicked with different concentrations of dodecanethiol and 3-mercaptopropionic acid; (a) 3 : 1 MPA/dodecanethiol, (b) 1 : 1 MPA/dodecanethiol and (c) 1 : 3 MPA/dodecanethiol. The characteristic bands for hydroxyl groups (COOH) of clicked MPA (peak between 3650 and 3050 cm^{-1}) and aliphatic groups (peaks at 2955, 2922 and 2853 cm^{-1}) of dodecanethiol clearly show the differences in the surface composition obtained at various thiol ratios. Quantitatively, the peak area ratio of peaks corresponding to hydroxyl groups (COOH) of MPA to the peaks corresponding to aliphatic groups of dodecanethiol ($A_{Peak,MPA}/A_{Peak,DDT}$) was observed to be 3.13, 0.71 and 0.14 for p(PgMA) functionalized with a mixture of MPA and dodecanethiol in the molar proportions of 3 : 1, 1 : 1, and 1 : 3. While $A_{Peak,MPA}/A_{Peak,DDT}$ values do not reflect the accurate concentrations of pendant COOH and aliphatic groups due to the contribution of aliphatic groups of p(PgMA) main chain and different extinction coefficients of the COOH and aliphatic groups, the relative comparison of $A_{Peak,MPA}/A_{Peak,DDT}$ values qualitatively suggest that it is straightforward to control the concentration of the functional groups, and in turn, the surface properties (wettability in our case) of p(PgMA) brush after thiol-yne reaction by simply varying the concentration of component thiols in the initial mixture.

Fig. 3 shows the wettability of the clicked polymer brush as a function of the initial MPA/dodecanethiol molar concentrations evaluated by water contact angle measurements after a final THF rinse. As expected, water contact angles of the dually-clicked MPA/dodecanethiol polymer brush lie between the water contact angles of polymer brushes clicked individually with MPA (52°) and dodecanethiol (101°), and decrease as the concentration of MPA in the MPA/dodecanethiol reaction mixture increases.

Additionally, methanol as a final rinse induces rearrangement of the top surface of the dual-functional brush, which exposes COOH groups at the surface. Thus, the water contact angles after the methanol rinse are lower than the water contact angles after THF rinsing treatment across the compositional series, but in general, both follow similar trends. Though the one-pot approach is an extremely simple method to synthesize dual or multi-functional brushes with tunable surface properties, it

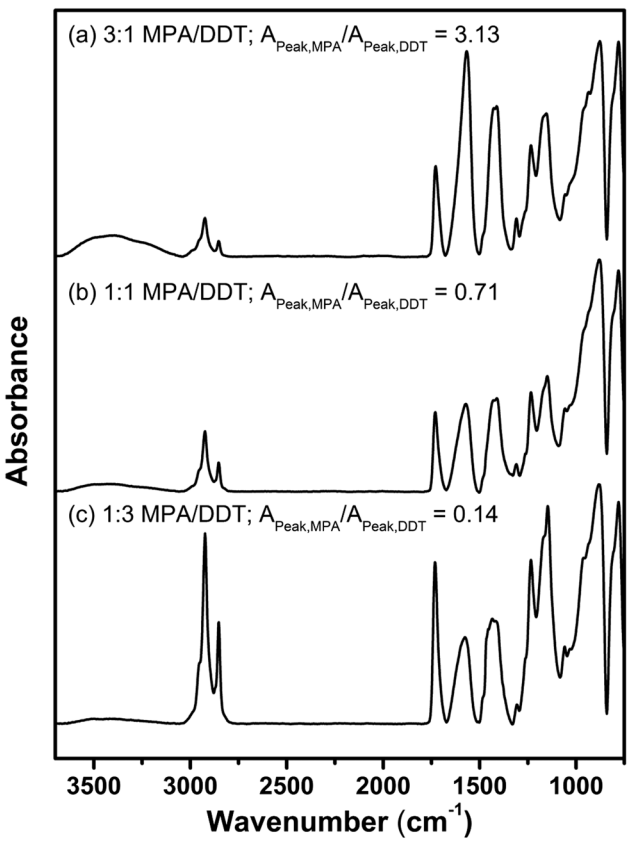

Fig. 2 p(PgMA) brush clicked with a mixture of mercaptopropionic acid (MPA) and dodecanethiol (DDT) in the ratio of a) 3 : 1, 32.1 nm ± 7.3 nm; b) 1 : 1, 38.3 nm ± 4.3 nm; and c) 1 : 3, 53.0 nm ±1.7 nm.

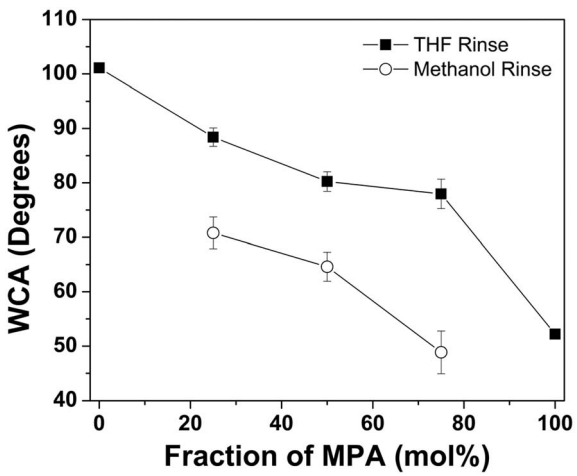

Fig. 3 Water contact angle of p(PgMA) brushes functionalized with 3-mercaptopropionic acid and dodecanethiol *via* one-pot thiol-yne reactions as a function of molar fraction of 3-mercaptopropionic acid in the thiol mixture. Error bars represent one standard deviation of the data, which is taken as the experimental uncertainty of the measurement. Some error bars are smaller than the symbols.

suffers from a limitation that one-pot thiol-yne reactions are random and non-specific, *i. e.* both functional groups are arranged randomly within the polymer brush and as a mixture of 1,2-homo and 1,2-hetero dithioether adducts. Additionally, the only control over surface composition of the clicked functional groups in this approach is the molar ratio of the thiols in the initial reaction mixture. In many cases, particularly where site-specific modifications are of interest and warranted, *i.e.* block copolymers, gradients, and patterned brush surfaces, it would be advantageous to explore sequential and/or orthogonal surface modification schemes.

Sequential/orthogonal click reactions for synthesis of multi-functional polymer brushes. Due to different mechanisms for reactions within the thiol-click toolbox, it is expected that nucleophile-mediated and radical-mediated reactions of thiols with various functional groups can be conducted in an orthogonal fashion. Indeed, the orthogonal nature of thiol-click reactions, in combination with other chemistries, has been previously harnessed by several authors to fabricate functional polymers,[46,47] surfaces,[48] dendrimers[49,50] and several other polymer architectures.[36,51] In this work, we specifically used the orthogonal nature of thiol-click reactions to fabricate dual-functional polymer brushes. Close examination of the thiol-click toolbox suggests that several pairs of thiol-clickable monomers can be used to synthesize dual-functional polymer brushes. Synthesis of these dual-functional brushes, as shown in Scheme 2, was performed by first synthesizing copolymer brushes *via* copolymerization of monomers containing two different thiol-clickable functional groups, followed by sequential and orthogonal thiol-click reactions. Taking advantage of the orthogonal nature of the radical-mediated thiol-yne reaction and nucleophilic reaction of thiols with isocyanates, alkylhalides, and epoxides, we synthesized copolymer brushes *via* SIP from mixtures of PgMA-TMS with NCOMA, BrMA and GMA to form p(NCOMA-stat-PgMA), p(BrMA-stat-PgMA) and p(GMA-stat-PgMA), respectively. In all cases, the nucleophilic thiol-isocyanate, thiol-halogen and thiol-epoxy reactions were performed first followed by deprotection of alkyne group and thiol-yne click reaction. It should be noted that protection of the alkyne group was necessary only to eliminate radical-mediated side reactions during the synthesis of copolymer brushes by SIP.

Orthogonal thiol-isocyanate and thiol-yne functionalization to form dual-functional polymer brush. SIP of NCOMA and PgMA-TMS was performed for 45 min at 150 mW cm^{-2} to synthesize p(NCOMA-stat-PgMA). Fig. 4(a) shows the gATR-FTIR spectrum for unmodified p(NCOMA-stat-PgMA). Peaks at 2180 cm^{-1} and 2275 cm^{-1} are attributed to the protected alkyne and isocyanate groups, respectively, confirming the presence of both alkyne and isocyanate groups in the statistical copolymer brush. While the ratio of isocyanate and alkyne groups in the copolymer brush could be varied simply by changing the ratio of NCOMA and PgMA-TMS in the monomer mixture, quantifying the ratios in the copolymer brush is beyond the scope of this study and will not be discussed in detail here. Due to the reactivity of isocyanate groups towards moisture, the p(NCOMA-stat-PgMA) surfaces were stored under nitrogen at room temperature until ready for further modification. Additionally, all thiol-isocyanate click reactions were performed using dry solvents. Tertiary amine catalysts facilitate rapid reactions *via* generation of 1) a more electron deficient carbonyl carbon within the isocyanate moiety and 2) a strongly nucleophilic thiolate ion.[52,53] In the first click reaction, benzyl mercaptan was reacted with isocyanate groups in the copolymer brush for 1 h. Fig. 4(b) shows the FTIR spectrum of p(NCOMA-stat-PgMA) brush after the thiol-isocyanate click reaction. The disappearance of the peak associated with the isocyanate group (2275 cm^{-1}) and appearance of peaks indicative of the thiourethane linkage (3326 cm^{-1} NH-CO) and incorporated benzyl mercaptan (3018 and 3030 cm^{-1} (=C–H); 1517, 1493 and 1451 cm^{-1} (C=C)) confirm the successful thiol-isocyanate reaction. Notably, the peak at 2180 cm^{-1} corresponding to the protected alkyne group was found to be intact following the thiol-isocyanate click reaction suggesting that thiol-isocyanate transformations do not affect the protected alkyne groups and can be utilized for further transformations to form a dual-functional polymer brush.

To perform the sequential thiol-yne reaction, alkyne groups must be deprotected to remove the trimethylsilyl functionality. Deprotection of the alkyne moieties under caustic conditions

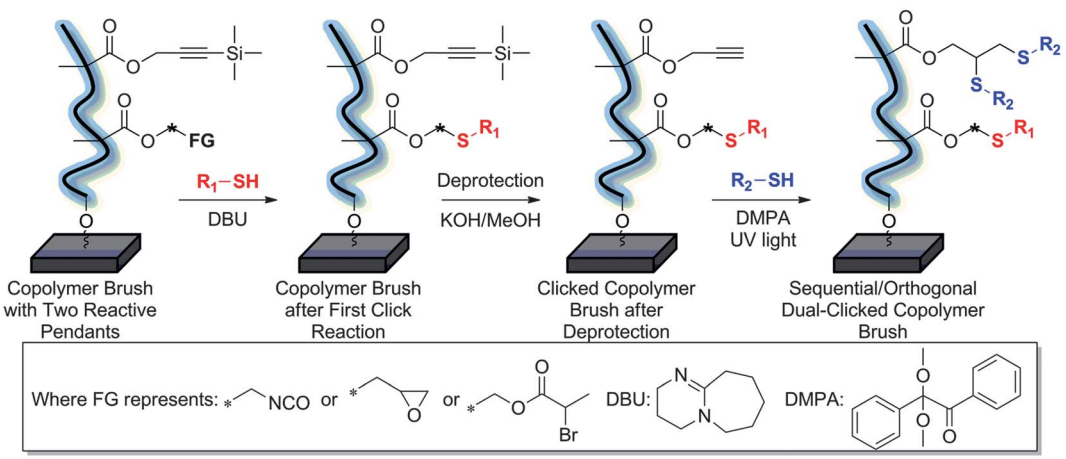

Scheme 2 Schematic for synthesis of dual-functional polymer brushes by sequential and orthogonal and thiol-based click reactions.

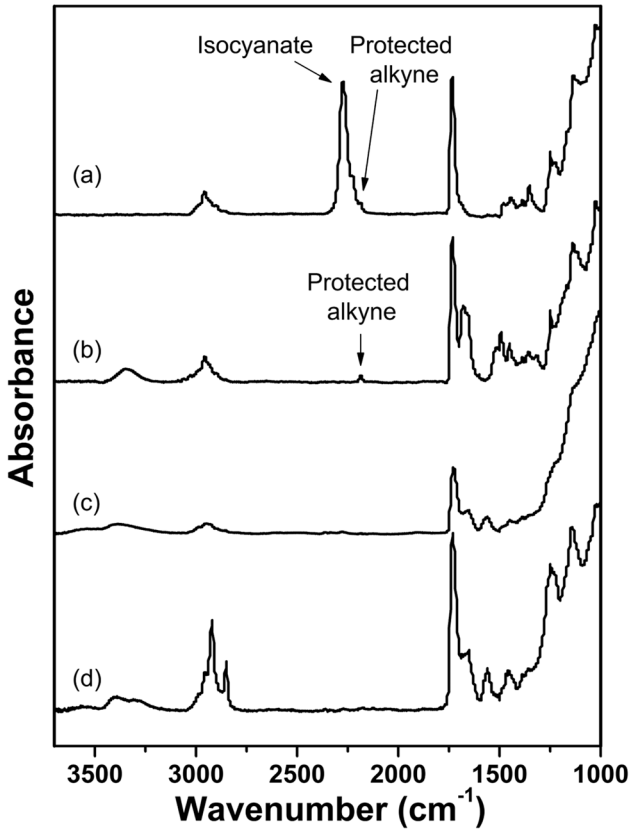

Fig. 4 a) gATR-FTIR spectra for p(NCOMA-stat-PgMA-TMS) synthesized by SIP of 1 : 6 v/v PgMA:NCOMA, 76.4 nm ± 2.8 nm; b) after thiol-isocyanate click with benzyl mercaptan, 125.9 nm ± 1.2 nm; c) after deprotection using AgOTf, 101.7 nm ± 1.8 nm; and d) after thiol-yne click with dodecanethiol, 127.1 nm ± 0.3 nm.

using KOH in methanol was first attempted. However, it was found that the thiourethane bonds resulting from the initial thiol-isocyanate click reaction are labile under these caustic conditions leading to loss of tethered functionality. To eliminate thiourethane cleavage, we adapted an alternate mild strategy to deprotect the alkyne group. In this method, p(NCOMA-stat-PgMA) brushes clicked with benzyl mercaptan were treated with silver triflate (AgOTf) overnight using THF/water (1 : 1 v/v) as solvent.[54] Fig. 4(c) shows the p(NCOMA-stat-PgMA) after the AgOTf-mediated deprotection step. The peak corresponding to the protected alkyne at 2180 cm^{-1} disappears after the treatment with AgOTf; however, the peak expected for deprotected alkyne at 2210 cm^{-1} was not observed. While the disappearance of the peak corresponding to the protected alkyne can be attributed to the formation of silver acetylide complex, it is crucial to understand the mechanism of AgOTf-mediated deprotection to understand the absence of deprotected alkyne peaks. Typically, in an AgOTf-mediated silyl deprotection shown in Scheme 3, the silver acetylide complex and triflic acid are formed upon silver activation of the alkyne and hydrolysis of the resulting Me_3SiOTf. This triflic acid then hydrolyzes the silver acetylide complex to give a deprotected alkyne and regenerates AgOTf.[54] However, in the case of deprotection of surface-tethered protected alkyne groups, we speculate triflic acid generated during the deprotection step quickly diffuses away from the polymer

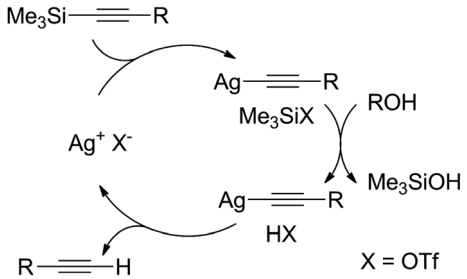

Scheme 3 General mechanism for Ag-mediated deprotection of trimethylsilyl-protected alkynes.[54] Diffusion of triflic acid out of the brush surface would result in incomplete deprotection and the presence of brush-bound silver acetylide.

brush surface into solution resulting in incomplete deprotection leaving alkyne groups in a silver acetylide form. High resolution XPS indeed shows the presence of silver with an Ag3d binding energy of 368.25 eV (see Supporting Information Figure S1†). We posit that regardless of the exact nature of the alkyne group after AgOTf-mediated deprotection, it should still be reactive in the subsequent thiol-yne reactions. To prove this, we performed the sequential radical-mediated thiol-yne reaction using dodecanethiol and DMPA on the AgOTf treated brushes. Fig. 4(d) shows the gATR-FTIR spectrum after thiol-yne reaction with dodecanethiol. As shown in Fig. 4(d), the appearance of peaks corresponding to aliphatic groups of dodecanethiol at 2955 cm^{-1}, 2922 cm^{-1} and 2853 cm^{-1} confirms the successful thiol-yne reaction (regardless of the speculated silver acetylide complex) and the successful sequential thiol-isocyanate/thiol-yne transformations of the p(NCOMA-stat-PgMA) brush. Although not ideal due to the fact that residual silver remains in the film even after thiol-yne modification (see Supporting Information Figure S1†), these results suggest that AgOTf-mediated deprotection of surface-tethered functional groups can be used as an alternative in cases where highly caustic conditions might pose a problem.

Orthogonal thiol-bromo and thiol-yne functionalization to form multifunctional polymer brushes. A methodology similar to that described previously for sequential thiol-isocyanate/thiol-yne surface reactions was adapted for the synthesis of statistical copolymer brushes comprised of BrMA and PgMA-TMS allowing for sequential thiol-bromo and thiol-yne transformations. In the case of thiol-bromo/thiol-yne surface reactions, the weak FTIR signature of the secondary bromine in pBrMA prevents the confirmation of the incorporated bromo functionality using gATR-FTIR spectroscopy. Rather, XPS was performed to follow the sequence of reactions for this system. Fig. 5(a) shows the survey and corresponding high resolution C1s, S2p, and Br3d spectra for a p(BrMA-stat-PgMA) brush prepared *via* SIP from a 1 : 1 mixture of BrMA and PgMA in THF. The C1s (285 eV), O1s (531 eV) and particularly the presence of bromine (Br3d, 70 eV; Br3p, 182 eV; Br3s, 257 eV) confirms the successful surface-initiated copolymerization. Due to the thickness (10.9 nm for the unmodified brush) of the polymer brush samples, signals from the silicon substrate (Si2p, 100 eV; Si2s, 149 eV) are also present. Evidence for the presence of the TMS-protected alkyne was confirmed by gATR-FTIR as

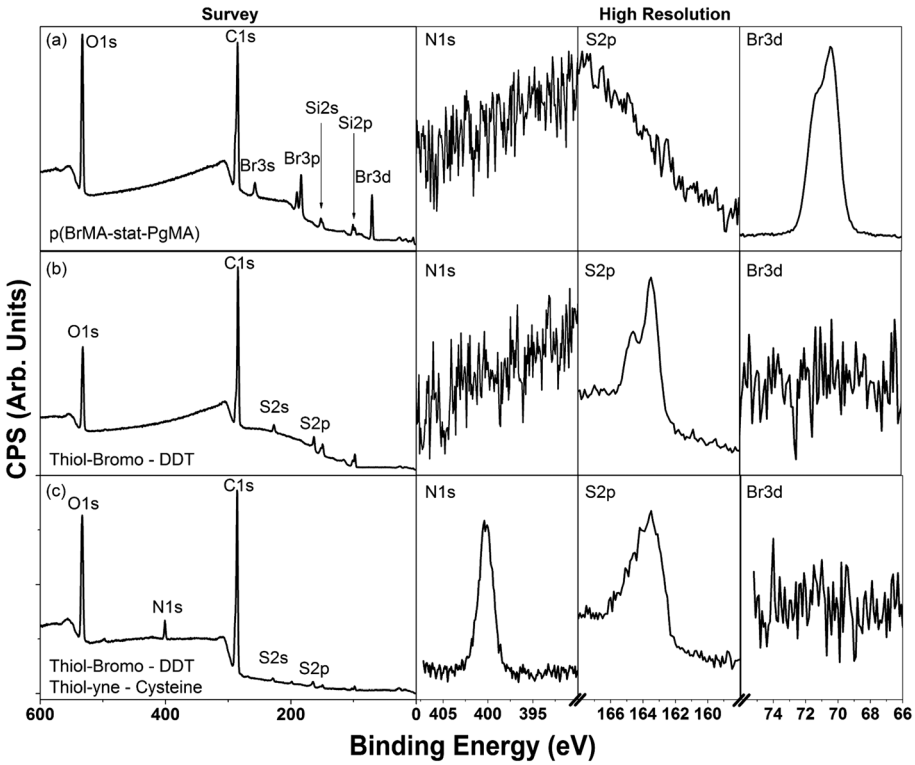

Fig. 5 Survey and N1s, S2p, and Br3d high-resolution XPS spectra for (a) unmodified statistical copolymer brush p(BrMA-stat-PgMa), 10.9 nm ± 1.2 nm; (b) p(BrMA-stat-PgMa) with α-bromoesters clicked with dodecanethiol (DDT), 25.5 nm ± 5.6 nm; and (c) p(BrMA-stat-PgMa) with α-bromoesters clicked with dodecanethiol and alkynes sequentially clicked with N-acetyl cysteine, 28.2 nm ± 4.8 nm.

previously described. Next, the α-bromo functional groups of p(BrMA-stat-PgMA) brush surface were modified with dodecanethiol under base-catalyzed (DBU) conditions. The disappearance of the peaks associated with bromine (Br3d, 70 eV; Br3p, 182 eV; Br3s, 257 eV) and the appearance of peaks attributed to sulfur (S2p, 163.4 eV; S2s, 229 eV) provide evidence for a successful replacement of bromine with the thioether (Fig. 5 (b)). An expected increase in the C/O ratio was also observed as a result of the incorporation of aliphatic dodecanethiol molecules. Again, the presence of the protected alkyne was confirmed by FTIR. After deprotection of the alkyne under KOH/methanol conditions, the alkyne pendants were modified by radical-mediated thiol-yne with *N*-acetyl cysteine as indicated by the appearance of the nitrogen N1s peak (400 eV) in Fig. 5(c). It is noteworthy that the preliminary investigations of thiol-bromo surface reactions were much slower when conducted under similar conditions of the thiol-isocyanate click reaction which reflects the difference in reactivity between the α-bromoester and isocyanate. Nonetheless, both systems reach quantitative conversion (within the sensitivity of our surface measurements) given sufficient reaction time.

Orthogonal thiol-epoxy and thiol-yne functionalization to form multifunctional polymer brushes. The thiol-epoxy reaction has recently been demonstrated as an efficient route to polymer modification.[38] Here, sequential thiol-epoxy and thiol-yne reactions on p(GMA-stat-PgMA) brushes were carried out under identical conditions as described above for the sequential thiol-bromo/thiol-yne system. p(GMA-stat-PgMA) brushes were synthesized by SIP from a mixture of GMA and PgMA-TMS. Varying the thickness and composition of the brushes (vide-infra) was easily achieved by changing the time of SIP and composition of monomer mixture, respectively. Fig. 6(a) shows the gATR-FTIR spectrum of p(GMA-stat-PgMA) synthesized by SIP from a equimolar mixture of GMA and PgMA in THF. The spectrum shows the characteristic peaks corresponding to epoxy ring at 906 cm^{-1} and protected alkyne at 2180 cm^{-1} confirming the presence of both epoxy and alkyne clickable moieties in the copolymer brush. Similar to the case of p(BrMA-stat-PgMA) and p(NCOMA-stat-PgMA), the tertiary amine-catalyzed thiol-epoxy transformation was performed first using thioglycerol and DBU. Fig. 6(b) shows the gATR-FTIR spectrum for thioglycerol-modified p(GMA-stat-PgMA) brush in which the thiolysis of the epoxy was confirmed by disappearance of an epoxy ring stretch at 906 cm^{-1}, and appearance of a strong, broad peak at 3400 cm^{-1} attributable to the hydroxyl groups of thioglycerol. Again, the peaks corresponding to the protected alkyne at 2180 cm^{-1} remain intact after the thiol-epoxy reaction. The thioglycerol-modified p(GMA-stat-PgMA) brush was then exposed to KOH/methanol to deprotect the TMS-alkyne group. Fig. 6(c) shows the p(GMA-stat-PgMA) after deprotection step indicating the disappearance of the protected alkyne group at 2180 cm^{-1} and appearance of peaks corresponding to the deprotected alkyne at 2230 cm^{-1} confirming successful deprotection under caustic conditions. Additionally, peaks corresponding to thioglycerol hydroxyl groups remain intact after deprotection step indicating that the thioether bond resulting from the thiol-epoxy reaction is stable under the caustic

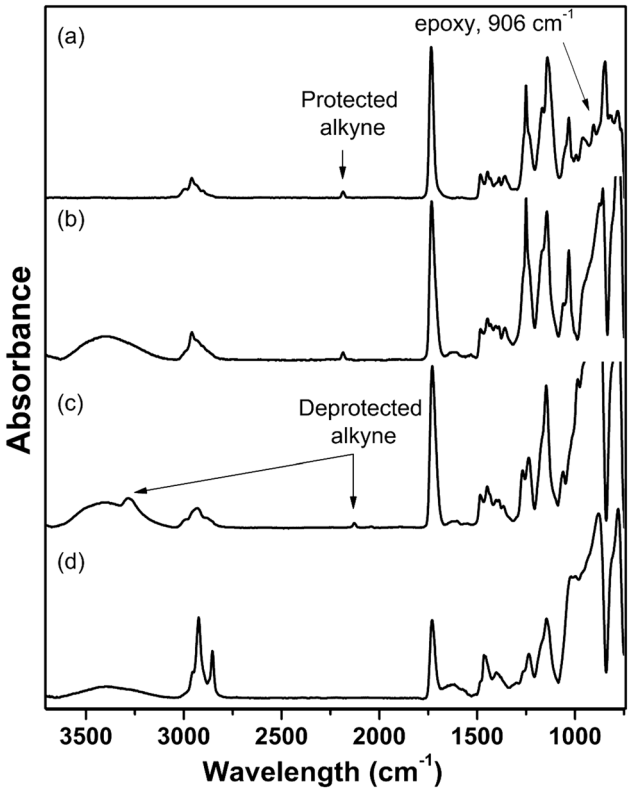

Fig. 6 gATR-FTIR spectrum for p(GMA-stat-PgMA) a) synthesized by SIP of 1 : 3 v/v GMA:PgMA, 73.5 nm ± 4.5 nm; b) after thiol-epoxy click with thioglycerol, 122.7 nm ±1.1 nm; c) after deprotection using KOH in methanol, 92.9 nm ± 5.8 nm; and d) after thiol-yne click with dodecanethiol, 126.2 nm ± 4.4 nm.

conditions, unlike the thiourethane bond discussed previously. Subsequently, the deprotected pendent alkyne groups were transformed by thiol-yne reaction using dodecanethiol as a model thiol. Fig. 6(d) shows the spectrum for the p(GMA-stat-PgMA) after final thiol-yne modification. The gATR-FTIR spectrum clearly confirms the thiol-yne click showing the sharp peaks at 2955, 2922 and 2853 cm^{-1} corresponding to aliphatic groups of dodecanethiol along with loss of peaks at 2125 and 3280 cm^{-1} corresponding to deprotected alkyne groups. Thus, a dual-functional brush containing hydroxyl and aliphatic groups was synthesized by sequential thiol-based reactions starting with a p(GMA-stat-PgMA) copolymer brush.

Taken together, these studies of functionalizing the copolymer brushes containing two thiol-clickable groups prove, in concept, that orthogonal thiol-click reactions can be conducted in a sequential manner to yield dual-functional polymer brushes. Though, for all three systems, only one type of thiol was used for each of the click reactions, it has been shown previously by numerous researchers that these thiol-click reactions can be conducted with a multitude of thiols imparting the desired properties to the polymer brush. Additionally, with the choice of two thiols, the properties of the surface can be tuned by varying the composition of copolymer brush (concentration of one thiol-clickable group relative to another thiol-clickable group). To demonstrate tunability of the copolymer brushes, we synthesized dual-functional polymer brushes of varying wettability by sequential and orthogonal click reactions from p(GMA-stat-PgMA).

Tuning surface properties *via* orthogonal click transformations. We have already demonstrated facile tunability of the composition and wetting properties of polymer brush surfaces using a one-pot thiol-yne approach with binary and ternary thiol mixtures. Similarly, it should be possible to impart tunability by controlling the functional monomer feed ratios used in the statistical copolymerization from the surface, which in turn dictates the final composition and properties of the surface upon sequential click reactions at full functional group conversion. To explore this concept, statistical copolymer brushes containing varying concentrations of epoxy and alkyne functionality were synthesized by SIP from different monomer feed ratios of GMA and PgMA. Fig. 7 (a–c) shows the FTIR spectra for copolymer brushes synthesized by SIP from different GMA/PgMA feed ratios containing 25% v/v, 50% v/v and 75% v/v GMA, respectively. As the concentration of GMA in monomer feed increases, the concentration of epoxy functionality relative to the alkyne functionality in the copolymer brush increases as indicated by an increase in the height of the peak at 906 cm^{-1} corresponding to the epoxy group and decrease in the height of the peak at 2180 cm^{-1} corresponding to the protected alkyne group. The trend in the concentration of epoxy and alkyne functionality in the copolymer brush was confirmed by calculating peak area ratios for epoxy and alkyne peaks ($A_{Peak,GMA}/A_{Peak,PgMA}$) in each of the FTIR spectra. As the fraction of GMA in monomer feed increases, $A_{Peak,GMA}/A_{Peak,PgMA}$ was calculated to be 1.70, 10.2, and 41.3 for copolymer brushes synthesized from 25% v/v, 50% v/v and 75% v/v GMA

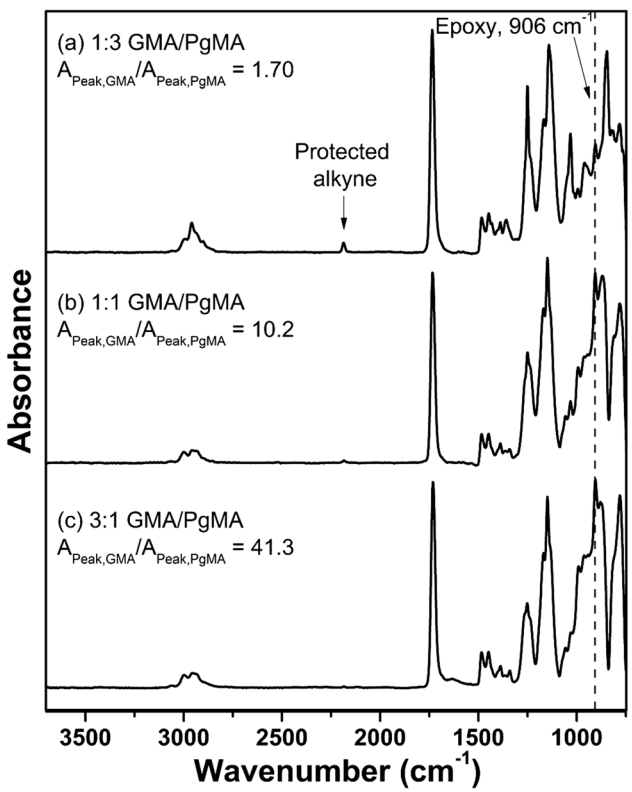

Fig. 7 gATR-FTIR spectra for p(GMA-stat-PgMA-TMS) synthesized by SIP of a) 1 : 3 v/v GMA:PgMA-TMS, 73.5 nm ± 4.5 nm; b) 1 : 1 v/v GMA:PgMA-TMS, 40.9 nm ± 2.1 nm; and c) 3 : 1 v/v GMA:PgMA-TMS, 68.2 nm ± 3.8 nm.

fractions, respectively. The variation in epoxy/alkyne composition in the copolymer brush was also characterized by water contact angle analysis. As shown in Fig. 8, the water contact angle of copolymer brush decreases from the observed value for pure pPgMA (96°) down to the observed for pure pGMA (56°) as the fraction of GMA in the monomer feed increases. This trend in the water contact angle is expected due to higher hydrophilicity of pGMA as compared to pPgMA. These p(GMA-stat-PgMA) surfaces were then employed as platforms for sequential thiol-epoxy and thiol-yne modifications in the same manner previously described. Due to the orthogonal nature of radical-mediated thiol-yne and base-catalyzed thiol-epoxy transformations, the p(GMA-stat-PgMA) copolymer brush can be modified with independent thiol-click reactions. To demonstrate control of surface properties, pendent epoxy groups were modified with hydrophilic thioglycerol, and pendent alkynes were modified with hydrophobic dodecanethiol. Fig. 9 shows the gATR-FTIR spectra of p(GMA-stat-PgMA) brushes clicked with thioglycerol and dodecanethiol *via* orthogonal thiol-epoxy and thiol-yne transformations, respectively. As the GMA fraction in the parent p(GMA-stat-PgMA) brush increases, the intensity of peaks corresponding to the hydroxyl groups at 3400 cm^{-1} increase as a result of the thiolysis of pendent epoxy moieties with thioglycerol. In contrast, after sequential thiol-yne click with dodecanethiol, the intensity of peaks corresponding to aliphatic groups at 2955, 2922 and 2853 cm^{-1} of dodecanethiol decreases as the fraction of GMA in the brush increases. Accordingly, as shown in Fig. 10, the water contact angle of the sequentially clicked copolymer brush surfaces decreases as the GMA fraction in the parent p(GMA-stat-PgMA) brush increases indicating the amount of hydrophilic thioglycerol and hydrophobic dodecanethiol incorporated in the brush is dictated simply from the composition of the parent polymer brush (assuming complete conversion of the epoxy and alkyne groups). Also shown in Fig. 10, the modified brush surfaces undergo rearrangement as a result of various solvent treatments. THF likely exposes a greater fraction of dodecanethiol at the surface, and *vice versa*, methanol likely exposes a greater fraction of thioglycerol. Although some degree of rearrangement is expected, we are particularly interested to probe the distribution of these functional groups in the depth direction of the polymer brush to learn more about the possibilities of creating unique polymer brush architectures with compositional gradients by exploiting

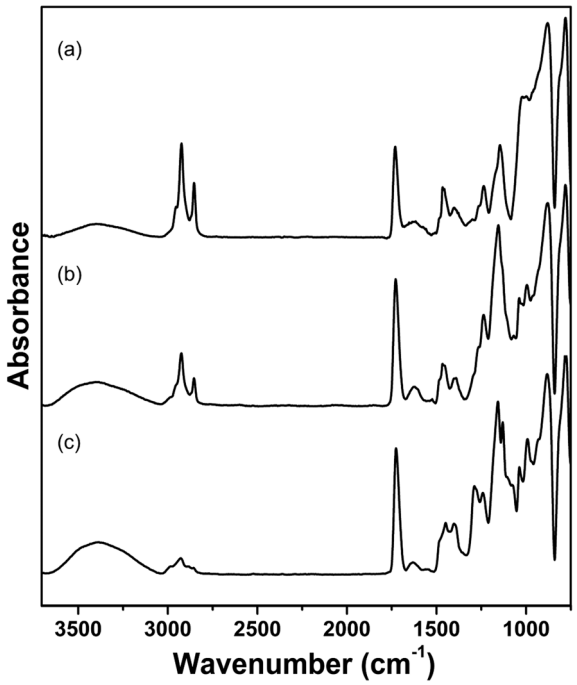

Fig. 9 gATR-FTIR spectra of p(GMA-stat-PgMA) after sequential thiol-epoxy and thiol-yne with thioglycerol and dodecanethiol, respectively. p(GMA-stat-PgMA) brushes are synthesized by SIP of a) 1 : 3 v/v GMA:PgMA, 54.2 nm ± 2.7 nm b) 1 : 1 v/v GMA:PgMA, 43.6 nm ± 1.2 nm; and c) 3 : 1 v/v GMA:PgMA, 48.4 nm ± 3.1 nm.

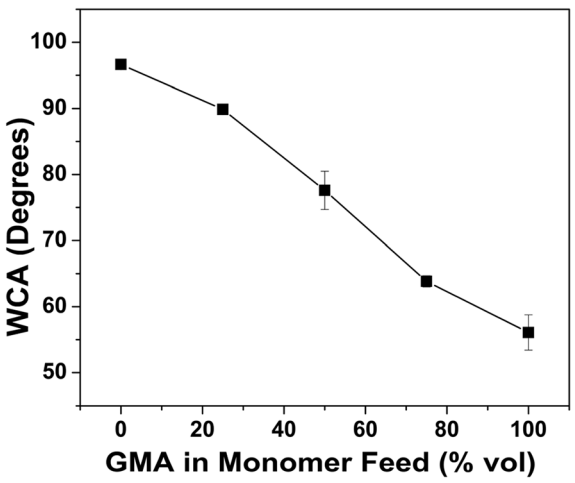

Fig. 8 Water contact angle of p(GMA-stat-PgMA) brushes as a function of GMA in the GMA/PgMA comonomer feed used for SIP. Error bars represent one standard deviation of the data, which is taken as the experimental uncertainty of the measurement. Some error bars are smaller than the symbols.

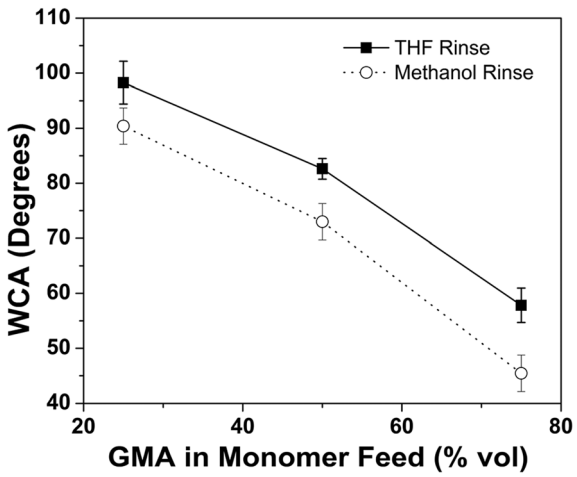

Fig. 10 Water contact angle of p(GMA-stat-PgMA) brushes clicked sequentially with thioglycerol and dodecanethiol *via* thiol-epoxy and thiol-yne reactions as a function of volume fraction of GMA in the GMA/PgMA monomer feed used for SIP. Error bars represent one standard deviation of the data, which is taken as the experimental uncertainty of the measurement.

size-dependent exclusion inherent to polymer brush systems. This work is currently underway.

Conclusions

In summary, we successfully demonstrated a versatile post-polymerization modification strategy to synthesize multifunctional polymer brush surfaces *via* combination of surface-initiated photopolymerization and orthogonal thiol-click reactions, namely the base-catalyzed thiol-isocyanate, thiol-epoxy, or thiol-bromo reactions in sequential combination with the radical-mediated thiol-yne reaction. Initially, the applicability of the radical-mediated thiol-yne reaction was extended to include one-pot statistical co-click reactions of brush pendant alkyne groups with multiple thiols. This simple one-pot approach was successfully applied to various mixtures of thiols including a combination of thioglycerol and dodecanethiol, which bestow hydrophilic hydroxyl and hydrophobic aliphatic groups to the polymer brush, respectively, and a combination of N-acetyl-cysteine and dodecanethiol to form a model polymer coating with a biologically relevant molecule. The one-pot approach was also shown to be easily extendable to a mixture of three thiols. The ability to control the surface properties (hydrophilicity in this work) by facile control over relative concentration of thiols in a thiol mixture also exhibits the robustness and versatility of the one-pot approach. Additionally, sequential and orthogonal thiol-click reactions were successfully applied to synthesize dual-functional polymer brushes by post-polymerization modification of p(NCOMA-stat-PgMA), p(GMA-stat-PgMA) and p(BrMA-stat-PgMA) *via* nucleophile-mediated thiol-isocyanate, thiol-epoxy or thiol-bromo, respectively, in combination with radical-mediated thiol-yne reactions. Generally, the base-catalyzed reactions were conducted first, and were observed to have no effect on the alkyne groups, which enabled the sequential thiol-yne reaction. In this case, surface properties were tailored by controlling the relative concentrations of monomers in the monomer feed during the SIP, which in turn dictates the composition of the thiol-clicked surface. While we demonstrated our strategy with model and commercially available thiols, we fully expect that this approach will be extended to fabrication of multiplexed biomolecules, *i.e.* proteins, DNA strands, antibodies, as well as the fabrication of complex polymer brush architectures, *i.e.* mixed and block copolymer brushes.

Acknowledgements

This work was supported in part by NSF CAREER (DMR-1056817) and the Office of Naval Research (Award N00014-07-1-1057). RMH acknowledges fellowship support from the U.S. Department of Education GAANN program (Award #P200A090066).

References

1 C. Sanchez, H. Arribart and M. M. Giraud Guille, *Nat. Mater.*, 2005, **4**, 277–288.
2 C. Hartmuth, M. Finn and B. Sharpless, *Angew. Chem., Int. Ed.*, 2001, **40**, 2004–2021.
3 L. Nebhani and C. Barner-Kowollik, *Adv. Mater.*, 2009, **21**, 3442–3468.
4 P. T. Dirlam, G. A. Strange, J. A. Orlicki, E. D. Wetzel and P. J. Costanzo, *Langmuir*, 2009, **26**, 3942–3948.
5 X.-L. Sun, C. L. Stabler, C. S. Cazalis and E. L. Chaikof, *Bioconjugate Chem.*, 2005, **17**, 52–57.
6 S. Arumugam and V. V. Popik, *J. Am. Chem. Soc.*, 2011, **133**, 15730–15736.
7 C. Hoyle, T. Lee and T. Roper, *J. Polym. Sci., Part A: Polym. Chem.*, 2004, **42**, 5301–5338.
8 C. E. Hoyle, A. B. Lowe and C. N. Bowman, *Chem. Soc. Rev.*, 2010, **39**, 1355–1387.
9 C. E. Hoyle and C. N. Bowman, *Angew. Chem., Int. Ed.*, 2010, **49**, 1540–1573.
10 A. B. Lowe, C. E. Hoyle and C. N. Bowman, *J. Mater. Chem.*, 2010, **20**, 4745–4750.
11 D. Kessler, K. Nilles and P. Theato, *J. Mater. Chem.*, 2009, **19**, 8184–8189.
12 H. Murata, O. Prucker and J. Rühe, *Macromolecules*, 2007, **40**, 5497–5503.
13 S. V. Orski, K. H. Fries, G. R. Sheppard and J. Locklin, *Langmuir*, 2010, **26**, 2136–2143.
14 R. K. Iha, K. L. Wooley, A. M. Nyström, D. J. Burke, M. J. Kade and C. J. Hawker, *Chem. Rev.*, 2009, **109**, 5620–5686.
15 K. L. Christman, E. Schopf, R. M. Broyer, R. C. Li, Y. Chen and H. D. Maynard, *J. Am. Chem. Soc.*, 2008, **131**, 521–527.
16 G. A. Hudalla and W. L. Murphy, *Langmuir*, 2010, **26**, 6449–6456.
17 S. Im, K. Bong, B.-S. Kim, S. Baxamusa, P. Hammond, P. Doyle and K. Gleason, *J. Am. Chem. Soc.*, 2008, **130**, 14424–14425.
18 J. M. Baskin, J. A. Prescher, S. T. Laughlin, N. J. Agard, P. V. Chang, I. A. Miller, A. Lo, J. A. Codelli and C. R. Bertozzi, *Proc. Natl. Acad. Sci. U. S. A.*, 2007, **104**, 16793–16797.
19 J. C. Jewett, E. M. Sletten and C. R. Bertozzi, *J. Am. Chem. Soc.*, 2010, **132**, 3688–3690.
20 R. Manova, T. A. van Beek and H. Zuilhof, *Angew. Chem., Int. Ed.*, 2011, **50**, 5428–5430.
21 A. Kuzmin, A. Poloukhtine, M. A. Wolfert and V. V. Popik, *Bioconjugate Chem.*, 2010, **21**, 2076–2085.
22 S. V. Orski, A. A. Poloukhtine, S. Arumugam, L. Mao, V. V. Popik and J. Locklin, *J. Am. Chem. Soc.*, 2010, **132**, 11024–11026.
23 X. Deng, C. Friedmann and J. Lahann, *Angew. Chem., Int. Ed.*, 2011, **50**, 6522–6526.
24 B. J. Sparks, J. G. Ray, D. A. Savin, C. M. Stafford and D. L. Patton, *Chem. Commun.*, 2011, **47**, 6245–6247.
25 T. Cai, R. Wang, K. G. Neoh and E. T. Kang, *Polym. Chem.*, 2011, **2**, 1849–1858.
26 P. Jonkheijm, D. Weinrich, M. Koehn, H. Engelkamp, P. Christianen, J. Kuhlmann, J. Maan, D. Nuesse, H. Schroeder, R. Wacker, R. Breinbauer, C. Niemeyer and H. Waldmann, *Angew. Chem., Int. Ed.*, 2008, **47**, 4421.
27 C. Wendeln, S. Rinnen, C. Schulz, H. F. Arlinghaus and B. J. Ravoo, *Langmuir*, 2010, **26**, 15966–15971.
28 M. Li, P. De, H. Li and B. S. Sumerlin, *Polym. Chem.*, 2010, **1**, 854–859.
29 R. M. Hensarling, V. A. Doughty, J. W. Chan and D. L. Patton, *J. Am. Chem. Soc.*, 2009, **131**, 14673–14675.
30 C. Wang, P. F. Ren, X. J. Huang, J. Wu and Z. K. Xu, *Chem. Commun.*, 2011, **47**, 3930–3932.
31 Y. Huang, Y. Zeng, J. Yang, Z. Zeng, F. Zhu and X. Chen, *Chem. Commun.*, 2011, **47**, 7509–7511.
32 D. Konkolewicz, S. Gaillard, A. G. West, Y. Y. Cheng, A. Gray-Weale, T. W. Schmidt, S. P. Nolan and S. Perrier, *Organometallics*, 2011, **30**, 1315–1318.
33 S. S. Naik, J. W. Chan, C. Comer, C. E. Hoyle and D. A. Savin, *Polym. Chem.*, 2011, **2**, 303–305.
34 R. M. Hensarling, S. B. Rahane, A. P. LeBlanc, B. J. Sparks, E. M. White, J. Locklin and D. L. Patton, *Polym. Chem.*, 2011, **2**, 88–90.
35 H. Li, B. Yu, H. Matsushima, C. E. Hoyle and A. B. Lowe, *Macromolecules*, 2009, **42**, 6537–6542.
36 J. W. Chan, C. E. Hoyle and A. B. Lowe, *J. Am. Chem. Soc.*, 2009, **131**, 5751–5753.
37 R. Barbey, L. Lavanant, D. Paripovic, N. Schüwer, C. Sugnaux, S. Tugulu and H. A. Klok, *Chem. Rev.*, 2009, **109**, 5437–5527.
38 M. A. Harvison, T. P. Davis and A. B. Lowe, *Polym. Chem.*, 2011, **2**, 1347–1354.
39 B. M. Rosen, G. Lligadas, C. Hahn and V. Percec, *J. Polym. Sci., Part A: Polym. Chem.*, 2009, **47**, 3931–3939.
40 B. M. Rosen, G. Lligadas, C. Hahn and V. Percec, *J. Polym. Sci., Part A: Polym. Chem.*, 2009, **47**, 3940–3948.

41 J. Xu, L. Tao, C. Boyer, A. B. Lowe and T. P. Davis, *Macromolecules*, 2010, **43**, 20–24.
42 C. Schuh, S. Santer, O. Prucker and J. Rühe, *Adv. Mater.*, 2009, **21**, 4706–4710.
43 C. Xu, T. Wu, C. M. Drain, J. D. Batteas and K. L. Beers, *Macromolecules*, 2004, **38**, 6–8.
44 M. Beinhoff, J. Frommer and K. R. Carter, *Chem. Mater.*, 2006, **18**, 3425–3431.
45 B. D. Fairbanks, E. A. Sims, K. S. Anseth and C. N. Bowman, *Macromolecules*, 2010, **43**, 4113–4119.
46 L. M. Campos, K. L. Killops, R. Sakai, J. M. J. Paulusse, D. Damiron, E. Drockenmuller, B. W. Messmore and C. J. Hawker, *Macromolecules*, 2008, **41**, 7063–7070.
47 K. Kempe, R. Hoogenboom, M. Jaeger and U. S. Schubert, *Macromolecules*, 2011, **44**, 6424–6432.
48 A. S. Goldmann, A. Walther, L. Nebhani, R. Joso, D. Ernst, K. Loos, C. Barner-Kowollik, L. Barner and A. H. E. Müller, *Macromolecules*, 2009, **42**, 3707–3714.
49 P. Antoni, M. J. Robb, L. Campos, M. Montanez, A. Hult, E. Malmström, M. Malkoch and C. J. Hawker, *Macromolecules*, 2010, **43**, 6625–6631.
50 K. L. Killops, L. M. Campos and C. J. Hawker, *J. Am. Chem. Soc.*, 2008, **130**, 5062–5064.
51 J. Han, B. Zhao, Y. Gao, A. Tang and C. Gao, *Polym. Chem.*, 2011, **2**, 2175–2178.
52 C. E. Hoyle, A. B. Lowe and C. N. Bowman, *Chem. Soc. Rev.*, 2010, **39**, 1355–1387.
53 J. Shin, H. Matsushima, C. M. Comer, C. N. Bowman and C. E. Hoyle, *Chem. Mater.*, 2010, **22**, 2616–2625.
54 A. Orsini, A. Vitérisi, A. Bodlenner, J.-M. Weibel and P. Pale, *Tetrahedron Lett.*, 2005, **46**, 2259–2262.